

# Rethinking Token-Mixing MLP for MLP-based Vision Backbone

Tan Yu, Xu Li, Yunfeng Cai, Mingming Sun, Ping Li

Cognitive Computing Lab  
Baidu Research

10900 NE 8th St. Bellevue, Washington 98004, USA

No.10 Xibeiwang East Road, Beijing 100193, China

{tanyu01,lixu13,caiyunfeng,sunmingming01,liping11}@baidu.com

**Abstract.** In the past decade, we have witnessed rapid progress in the machine vision backbone. By introducing the inductive bias from the image processing, convolution neural network (CNN) has achieved excellent performance in numerous computer vision tasks and has been established as *de facto* backbone. In recent years, inspired by the great success achieved by Transformer in NLP tasks, vision Transformer models emerge. Using much less inductive bias, they have achieved promising performance in computer vision tasks compared with their CNN counterparts. More recently, researchers investigate using the pure-MLP architecture to build the vision backbone to further reduce the inductive bias, achieving good performance. The pure-MLP backbone is built upon channel-mixing MLPs to fuse the channels and token-mixing MLPs for communications between patches. In this paper, we re-think the design of the token-mixing MLP. We discover that token-mixing MLPs in existing MLP-based backbones are spatial-specific, and thus it is sensitive to spatial translation. Meanwhile, the channel-agnostic property of the existing token-mixing MLPs limits their capability in mixing tokens. To overcome those limitations, we propose an improved structure termed as Circulant Channel-Specific (CCS) token-mixing MLP, which is spatial-invariant and channel-specific. It takes fewer parameters but achieves higher classification accuracy on ImageNet1K benchmark.

## 1 Introduction

Convolution neural network (CNN) [20,13] has been *de facto* backbone for computer vision in the past years. Recently, inspired by the accomplishment achieved by Transformer [34] in NLP, several vision Transformer methods emerge [9,32]. Compared with CNN, vision Transformer methods do not need hand-crafted convolution kernels and simply stack a few Transformer blocks. Albeit vision Transformer methods take much less inductive bias, they have achieved comparable or even better recognition accuracy than CNN models. More recently, researchers have taken a step forward. They propose MLP-based models [30,31,25] with only MLP layers taking even less inductive bias.

MLP-mixer [30] is the pioneering work of pure-MLP vision backbone. It is built on two types of MLP layers: the channel-mixing MLP layer and the token-mixing MLP layer. The channel-mixing MLP is for communications between the channels. In parallel, the token-mixing MLP conducts communications between patches. Compared with vision Transformer adaptively assigning attention based on the relations between patches, the token-mixing MLP assigns fixed attention to patches based on their spatial locations. In fact, the channel-mixing MLP is closely related with depthwise convolution [4,17,19]. The differences between token-mixing MLP and depthwise convolution are three-fold. Firstly, the token-mixing MLP has a global reception field but the depthwise convolution has only a local reception field. The global reception field enables the token-mixer MLP to have access to the whole visual content in the image. Secondly, the depthwise convolution is spatial-invariant, whereas the channel-mixing MLP no longer possesses the spatial-invariant property and thus its output is sensitive to spatial translation. Lastly, for a specific position, the token-mixing MLP assigns an identical weight to elements in different channels. In contrast, the depthwise convolution applies different convolution kernels on different channels for encoding richer visual patterns.

Observing the strength and weakness of the vanilla token-mixing MLP in existing MLP-based backbones, we propose an improved structure, the Circulant Channel-Specific (CCS) token-mixing MLP which preserves the strength of the existing token-mixing MLP and overcomes its weakness. Similar to the vanilla token-mixing MLP, our CCS token-mixing MLP has a global reception field. Meanwhile, we adopt a circulant structure in the weight matrix to achieve the spatial-invariant property. Moreover, we adopt a channel-specific design to exploit richer manners in mixing tokens. In Table 1, we compare the properties of our CCS with depthwise convolution and vanilla token-mixing MLP. Moreover, benefited from circulant structure, our CCS needs considerably fewer parameters than the token-mixing MLP. To be specific, CCS only needs  $GN$  parameters where  $N$  is the number of patches and  $G$  is the number of groups. In contrast, the token-mixing MLP normally takes  $N^2$  parameters, which are significantly more than CCS since  $G \ll N$ . By replacing the token-mixing MLP with the proposed CCS in two existing pure-MLP vision backbones, we achieve consistently higher recognition accuracy on ImageNet1K with fewer parameters.

Property	Reception	Spatial	Channel
Depthwise	local	agnostic	specific
Token-mixing	global	specific	agnostic
CSC	global	agnostic	group-specific

**Table 1.** The properties of depthwise convolution, the token-mixing MLP in MLP-mixer [30] and our Circulant Channel-Specific (CCS) token-mixing MLP.

## 2 Related Work

### 2.1 Vision Transformer

Vision Transformer (ViT) [9] is the pioneering work adopting the architecture solely with Transformer layers for computer vision tasks. It crops an image into non-overlap patches and feeds these patches through a stack of Transformer layers for attaining communications between patches. Using less hand-crafted design, ViT achieves competitive recognition accuracy compared with its CNN counterparts. Nevertheless, it requires a huge scale of images for pre-training. DeiT [32] adopts a more advanced data augmentation method as well as a stronger optimizer, achieving excellent performance through training on a medium-scale dataset. PVT [35] introduces a progressive shrinking pyramid into ViT, improving the recognition accuracy. PiT [15] integrates depthwise convolution between Transformer blocks and also devises a shrinking pyramid structure. In parallel, Tokens-to-Tokens ViT [39] effectively models the local structure through recursively aggregating neighboring tokens. It achieves higher recognition accuracy with fewer FLOPs. Transformer-iN-Transformer (TNT) [12] also focuses on modeling the local structure. It devises an additional Transformer to model the intrinsic structure information inside each patch. Recently, the focus of vision Transformer is on improving efficiency through exploiting locality and sparsity. For instance, Swin [23] develops a hierarchical backbone with local-window Transformer layers with variable window sizes. Exploiting local windows considerably improves the efficiency, and the variable window scopes achieve the global reception field. Twins [5] alternately stacks a local-dense Transformer and a global-sparse Transformer, also achieving a global reception field in an efficient manner. Shuffle Transformer [18] also adopts the local-window Transformer and achieves the cross-window connections through spatially shuffling. S<sup>2</sup>ViTE [3] explores on integrating sparsity in vision Transformer and improves the efficiency from both model and data perspectives. Recent works [10,37] investigate combining convolution and Transformer to build a hybrid vision backbone.

### 2.2 MLP-based Backbone

Recently, MLP-mixer [30] proposes a pure-MLP backbone with less inductive bias than vision Transformer and CNNs, achieving excellent performance in image recognition. It is built upon two types of MLP layers: the channel-mixing MLP and the token-mixing MLP. The channel-mixing MLP is equivalent to  $1 \times 1$  convolution layer. It achieves the communications between channels. The token-mixing MLP achieves cross-patch communications. It is similar to the self-attention block in Transformer. But the attention in Transformer is dependent on the input patches, whereas the attention in the token-mixing MLP is agnostic to the input. Feed-forward (FF) [25] adopts a similar architecture as MLP-mixer, also achieving excellent performance. ResMLP [31] simplifies the token-mixing MLP in MLP-mixer and adopts a deep architecture stacking a huge number of layers. Meanwhile, to stabilize the training, ResMLP proposes an affine transform

layer to replace the layer normalization in MLP-mixer. Benefited from exploiting a deeper architecture, ResMLP achieves a better performance than MLP-mixer. Meanwhile, by smartly trading off the hidden size and depth, ResMLP takes fewer FLOPs and fewer parameters than MLP-mixer. Recently, gMLP [22] exploits a gating operation to enhance the effectiveness of the token-mixing MLP, attaining a higher recognition accuracy than MLP-mixer. In parallel, External Attention [11] replaces the self-attention operation with the attention on external memory implemented by fully-connected layers, achieving comparable performance with vision Transformers. Recently, spatial-shift MLP (S<sup>2</sup>MLP) [38] adopts a spatial-shift operation [36,2] to achieve the communications between patches, achieving excellent performance.

### 3 Preliminary

In this section, we briefly review the existing mainstream MLP backbone, MLP-Mixer [30]. It consists of three modules including a per-patch fully-connected layer, a stack of  $N$  Mixer layers, and a fully-connected layer for classification.

**Input.** For an input image of the size  $W \times H \times 3$ , we crop it into  $N$  non-overlap patches of  $p \times p \times 3$  size. For each patch, it is unfolded into a vector  $\mathbf{p} \in \mathbb{R}^{3p^2}$ . In total, we obtain a set of patch feature vectors  $\mathcal{P} = \{\mathbf{p}_0, \dots, \mathbf{p}_{N-1}\}$ , which are the input of the MLP-Mixer.

**Per-patch fully-connected layer.** For each patch feature  $\mathbf{p}_i \in \mathcal{P}$ , the per-patch fully-connected layer maps it into a  $C$ -dimensional vector by

$$\mathbf{x}_i \leftarrow \mathbf{W}_0 \mathbf{p}_i + \mathbf{b}_0, \quad (1)$$

where  $\mathbf{W}_0 \in \mathbb{R}^{3p^2 \times C}$  and  $\mathbf{b}_0 \in \mathbb{R}^C$  are the weights of the per-patch fully-connected layer.

**Mixer layers.** MLP-mixer stacks  $L$  mixer layers of the same size, and each layer contains two MLP blocks: the token-mixing MLP block and the channel-mixing MLP block. Let us denote the patch features in the input of each mixer layer as  $\mathbf{X} = [\mathbf{x}_0, \dots, \mathbf{x}_{N-1}] \in \mathbb{R}^{C \times N}$  where  $C$  is the number of channels and  $N$  is the number of patches. Channel-mixing block projects patch features  $\mathbf{X}$  along the channel dimension by

$$\mathbf{U} = \mathbf{U} + \mathbf{W}_2 \sigma[\mathbf{W}_1 \text{LayerNorm}(\mathbf{X})]. \quad (2)$$

$\mathbf{W}_1 \in \mathbb{R}^{rC \times C}$  represents weights of a fully-connected layer increasing the feature dimension from  $C$  to  $rC$  where  $r > 1$  is the expansion ratio.  $\mathbf{W}_2 \in \mathbb{R}^{C \times rC}$  denotes weights of a fully-connected layer decreasing the feature dimension from  $rC$  back to  $C$ . LayerNorm( $\cdot$ ) denotes the layer normalization [1] widely used in Transformer-based models and  $\sigma(\cdot)$  denotes the activation function implemented

by GELU [14]. Then the output of the channel-mixing block  $\mathbf{U}$  is fed into the token-mixing block for communications between patches:

$$\mathbf{Y} = \mathbf{U} + \sigma[\text{LayerNorm}(\mathbf{U})\mathbf{W}_3]\mathbf{W}_4, \quad (3)$$

where  $\mathbf{W}_3 \in \mathbb{R}^{N \times M}$  and  $\mathbf{W}_4 \in \mathbb{R}^{M \times N}$  denote the weights of fully-connected layers projecting patch features  $\mathbf{U}$  along the token dimension. Recently, ResMLP [31] adopts a simplified token-mixing block:

$$\mathbf{Y} = \mathbf{U} + \text{LayerNorm}(\mathbf{U})\mathbf{W}_3, \quad (4)$$

where  $\mathbf{W}_3 \in \mathbb{R}^{N \times N}$  is a square matrix. The experiments in ResMLP [31] show that the simplified token-mixing block achieves comparable performance as the original one defined in Eq. (3). Unless otherwise specified, the token-mixing we mention below is the simplified form defined in Eq. (4).

**Classification head.** After a stack of  $L$  mixer layers,  $N$  patches features are generated. They are further aggregated into a global vector through average pooling. Then the global vector is fed into a fully-connected layer for classification.

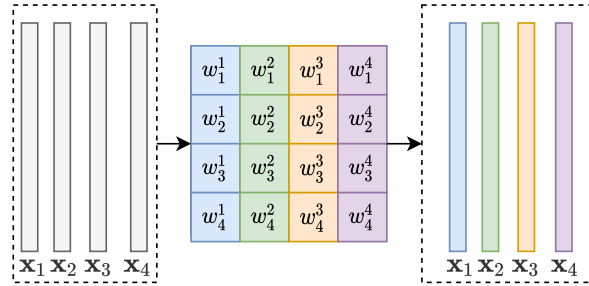
## 4 Circulant Channel-Specific Token-mixing MLP

In this section, we introduce our circulant channel-specific (CCS) token-mixing MLP. As we mention in the introduction, the vanilla token-mixing MLPs in MLP-mixer and ResMLP are spatial-specific and channel-agnostic. The spatial-specific property makes the token-mixing MLP sensitive to spatial translation. Meanwhile, the channel-agnostic configuration limits its capability in mixing tokens. The motivation of designing CCS token-mixing MLP is to achieve the spatial-agnostic property and meanwhile attain a channel-specific configuration for mixing tokens in a more effective way. To this end, we make two modifications to the vanilla token-mixing MLP, as illustrated in Figure 1, Algorithm 1, and details below.

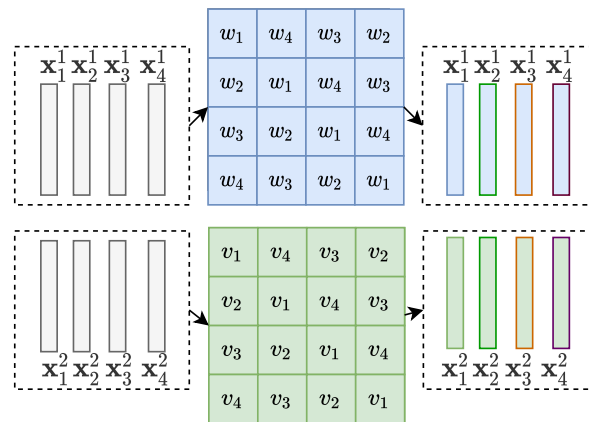
### 4.1 Circulant structure

We devise the weight matrix  $\mathbf{W}_3$  in Eq. (4) in a circulant structure. To be specific, we set the weight matrix  $\mathbf{W}_3$  in the below form:

$$\mathbf{W}_3 = \begin{bmatrix} w_0 & w_{N-1} & w_{N-2} & \dots & w_2 & w_1 \\ w_1 & w_0 & w_{N-1} & \dots & w_3 & w_2 \\ w_2 & w_1 & w_0 & \dots & w_4 & w_3 \\ \vdots & \vdots & \vdots & \ddots & \vdots & \vdots \\ w_{N-2} & w_{N-3} & w_{N-4} & \dots & w_0 & w_{N-1} \\ w_{N-1} & w_{N-2} & w_{N-3} & \dots & w_1 & w_0 \end{bmatrix}. \quad (5)$$



(a) Vanilla token-mixing MLP.



(b) Our CCS.

**Fig. 1.** Comparisons between vanilla token-mixing MLP in existing MLP-based backbones and the proposed Circulant Channel-Specific (CCS) token-mixing MLP. The proposed CCS imposes a circulant-structure constraint on the weights of the token-mixing MLP. Meanwhile, our CCS splits the input  $\mathbf{X}$  into multiple groups along the channel dimension. It uses different weight matrices on different groups for mixing tokens in a more flexible way.

It is fully specified by one vector,  $\mathbf{w} = [w_0, \dots, w_{N-1}]$ , which appears as the first column of  $\mathbf{W}_3$ . The circulant structure is naturally spatial-agnostic for mixing tokens. Below we show it in detail. Let us denote LayerNorm( $\mathbf{U}$ ) in Eq. (4) by  $\hat{\mathbf{U}} = [\hat{\mathbf{u}}_0, \dots, \hat{\mathbf{u}}_{N-1}]$ , where each item  $\hat{\mathbf{u}}_i$  ( $i \in [0, N-1]$ ) is the patch feature after layer normalization. We rewrite Eq. (4) into

$$\mathbf{Y} = \mathbf{U} + \hat{\mathbf{U}}\mathbf{W}_3. \quad (6)$$

Let us denote the  $i$ -th column of  $\hat{\mathbf{U}}$  by  $\hat{\mathbf{u}}_i$  and the  $i$ -th column of  $\hat{\mathbf{U}}\mathbf{W}_3$  by  $\bar{\mathbf{u}}_i$ . Then it is straightforward to obtain that

$$\bar{\mathbf{u}}_i = \sum_{j=0}^{N-1} w_j \hat{\mathbf{u}}_{(i+j)\%N}, \forall i \in [0, N-1], \quad (7)$$

---

**Algorithm 1** Pseudocode of our Circulant Channel-Specific (CCS) token-mixing MLP.

---

```

class CCS(nn.Module):
    def __init__(self, groups, patches):
        super().__init__()
        self.groups = groups
        self.w = nn.Linear(patches, self.groups).weight
    def forward(self, x):
        B, N, C = x.shape
        x = ifft(x, dim=1)
        w = fft(self.w, dim=1).unsqueeze(0).unsqueeze(2).expand(B, N, C // self
            .groups, self.groups).reshape(B, N, C)
        x = x.mul(w)
        x = fft(x, dim=1).real
        return x

```

---

where  $\%$  denotes the modulo operation. As shown in Eq. (7), the mixing operation for obtaining each patch feature  $\hat{\mathbf{u}}_i$  is invariant to the location  $i$ . Thus, the token-mixing MLP with the circulant-structure  $\mathbf{W}_3$  is spatial-agnostic, which is not sensitive to spatial translation. Meanwhile, the circulant structure reduces the number of parameters from  $N^2$  to  $N$ . At the same time, the multiplications between a  $N$ -dimension vector and an  $N \times N$  circulant matrix only take  $\mathcal{O}(N \log N)$  complexity using fast Fourier transform (FFT), which is more efficient than the vanilla vector-matrix multiplication with  $\mathcal{O}(N^2)$  computational complexity. Specifically, given an vector  $\mathbf{x} \in \mathbb{R}^N$  and a circulant matrix  $\mathbf{W}$  with the first column  $\mathbf{w}$ , the matrix-vector multiplication  $\mathbf{W}\mathbf{x}$  can be computed efficiently through

$$\mathbf{x}\mathbf{W} = \text{FFT}[\text{IFFT}(\mathbf{x}) \odot \text{FFT}(\mathbf{w})], \quad (8)$$

where FFT denotes fast Fourier transform, IFFT denotes inverse fast Fourier transform, and  $\odot$  denotes the element-wise product. Since both FFT and IFFT take only  $\mathcal{O}(N \log N)$  computational complexity, the total complexity is only  $\mathcal{O}(N \log N)$ . In contrast, the vanilla token-mixing MLP in existing methods takes  $\mathcal{O}(N^2)$  computational complexity. But when the number of patches,  $N$ , is not large, FFT with  $\mathcal{O}(N \log N)$  complexity can not demonstrate its efficiency advantage over the vanilla token-mixing MLP with  $\mathcal{O}(N^2)$  complexity.

## 4.2 Channel-Specific settings

The token-mixing MLP in MLP-mixer [30] shares the same weight among different channels. That is, the same token-mixing MLP is applied to each of  $C$  channels in  $\hat{\mathbf{U}} \in \mathbb{R}^{C \times N}$ . A straightforward extension is to devise  $C$  separable MLPs, namely,  $\{\text{MLP}_c\}_{c=1}^C$ . For each slide of  $\hat{\mathbf{U}}$  along the channel,  $\mathbf{U}[c, :] \in \mathbb{R}^N$ , it is processed by a specific  $\text{MLP}_c$ . This straightforward extension increases the number of parameters in the vanilla token-mixing MLP of MLP-mixer from  $N^2$

to  $N^2C$ . But the number of parameters,  $N^2C$ , is extremely huge, making the network prone to over-fitting. Thus, it does not bring noticeable improvements in the recognition accuracy, as claimed in the supplementary material of MLP-mixer [30].

In contrast, in our circulant-structure settings, even if we adopt  $C$  separable MLPs to process different channels of  $\hat{\mathbf{U}}$ , the number of parameters only increases from  $N$  to  $NC$ . The number of parameters is still on a medium scale. Thus, as shown in our experiments, using  $C$  separable circulant-structure MLPs can achieve better performance than that with a single circulant-structure MLP. To further reduce the number of parameters, we split  $C$  channels into  $G$  groups and each group contains  $C/G$  channels. For each group, we use a specific MLP. Thus, in this configuration, the number of parameters of our circulant-structure token-mixing MLP increases to  $GN$ , which is still significantly fewer than  $N^2$  parameters in vanilla MLP-mixing MLP since  $G \ll N$ . It is worth noting that, the computational complexity of our CCS token-mixing MLP is irrelevant to the number of groups,  $G$ . Thus, using  $G$  MLPs in token-mixing does not bring more computational cost than using a single MLP. We visualize the architecture of the vanilla token-mixing MLP and our CCS token-mixing MLP in Figure 1. We compare our CCS with the vanilla token-mixing MLP in Table 2. As shown in the table, our CCS token-mixing MLP takes fewer parameters than the vanilla token-mixing. We give the pseudocode of the proposed CCS token-mixing MLP in Algorithm 1.

settings	# of parameters	computational complexity
token-mixing	$N^2$	$N^2C$
CCS (ours)	$GN$	$N\log NC$

**Table 2.** Comparisons between our CCS and the vanilla token-mixing MLP on the number of parameters and computational complexity.  $N$  is the number of patches,  $C$  is the number of channels, and  $G$  denotes the number of groups, where  $G \ll N$ .

## 5 Experiments

**Datasets.** The main results are on ImageNet1K dataset [8]. It contains 1.2 million images from one thousand categories for training and 50 thousand images for validation. Note that MLP-mixer and ResMLP also exploit larger-scale datasets including ImageNet21K [8] and JFT-300M [27] datasets. Nevertheless, due to limited computing resources, it is impractical for us to train our models on these two datasets.

**Settings.** Our training follows the settings in DeiT [32]. To be specific, we adopt AdamW [24] as the optimizer with weight decay 0.05. A linear warm-up process is conducted at the beginning of training. The learning rate is initially

default settings	$N$	$L$	$C$	$r$	$p$	$G$	parameters
Mixer-B/16 [30] + CCS	196	12	768	4	16	8	57M
ResMLP-36 [31] + CCS	196	36	384	4	16	8	43M

**Table 3.**  $N$  is the number of tokens,  $L$  is the number of blocks,  $C$  is the hidden size,  $r$  is the expansion ratio,  $p$  is the patch size, and  $G$  is the number of groups in Table 2.

1e-3 and gradually drops to 1e-5 in a cosine-decay manner. We utilize multiple data augmentation approaches including random crop, random clip, Rand-Augment [7], Mixup [41] and CutMix [40]. Besides, we use replace dropout with DropPath [21] and conduct label smoothing [28] and repeated augmentation [16]. The whole training process takes 300 epochs. We integrate the proposed CCS token-mixing MLP in two types of mainstream MLP-based backbones including Mixer-B/16 [30] and ResMLP-36 [31]. Specifically, we only replace the vanilla token-mixing MLP with the proposed CCS token-mixing MLP and keep other layers unchanged. Table 3 provides the detailed settings for these two backbones. The code will be available based on the PaddlePaddle deep learning platform.

## 5.1 Main experimental results

The main experimental results are presented in Table 4. We compare ours with existing CNN-based models, Transformer-based models and MLP-based models. The first part of Table 4 contains the CNN-based models, including the classic ResNet-50 [13] and the recent state-of-the-art methods such as RegNetY-16GF [26], EfficientNet-B3 [29] and EfficientNet-B5 [29]. Note that, the architectures of RegNetY-16GF, EfficientNet-B3 and EfficientNet-B5 are all attained based on network architecture search (NAS). The main strength of EfficientNet is excellent recognition accuracy with the extremely cheap computational cost.

The second group of methods is based on vision Transformer. ViT [9] is the pioneering work with architecture solely based on Transformer. We show its performance with extra regularization reported in MLP-mixer [30], which is better than the performance in the original ViT paper. DeiT [32] adopts more advanced optimizer and data augmentation approaches, achieving considerably better performance than ViT. The following works including TNT [12] and T2T [39] enhance the effectiveness of modeling local structure, achieving better performance. In parallel, PVT [35] and PiT [15] adopt a pyramid structure following CNNs, also attaining higher accuracy than DeiT and ViT. CPVT [6] improves the positional encoding. CaiT [33] investigates deeper structures. Swin [23] exploits the locality, achieving higher efficiency. Container [10] proposes a hybrid architecture that exploits both convolution and Transformer, achieving excellent accuracy and efficiency. Compared with the CNN-based methods, methods based on vision Transformer have achieved comparable or even better performance. Besides, Transformer-based methods need less inductive bias, which is more friendly to network architecture search (NAS).

Model	Resolution	Top-1 (%)	Top5 (%)	Params (M)	FLOPs (B)
CNN-based methods					
ResNet50 [13]	$224 \times 224$	76.2	92.9	25.6	4.1
RegNetY-16GF [26]	$224 \times 224$	80.4	–	83.6	15.9
EfficientNet-B3 [29]	$300 \times 300$	81.6	95.7	12	1.8
EfficientNet-B5 [29]	$456 \times 456$	84.0	96.8	30	9.9
Transformer-based methods					
ViT-B/16* [9,30]	$224 \times 224$	79.7	–	86.4	17.6
DeiT-B/16 [32]	$224 \times 224$	81.8	–	86.4	17.6
PVT-L [35]	$224 \times 224$	82.3	–	61.4	9.8
TNT-B [12]	$224 \times 224$	82.8	96.3	65.6	14.1
T2T-24 [39]	$224 \times 224$	82.6	–	65.1	15.0
CPVT-B [6]	$224 \times 224$	82.3	–	88	17.6
PiT-B/16 [15]	$224 \times 224$	82.0	–	73.8	12.5
CaiT-S32 [33]	$224 \times 224$	83.3	–	68	13.9
Swin-B [23]	$224 \times 224$	83.3	–	88	15.4
Nest-B [42]	$224 \times 224$	83.8	–	68	17.9
Container [10]	$224 \times 224$	82.7	–	22.1	8.1
MLP-based methods					
FF [25]	$224 \times 224$	74.9	–	59	12
S <sup>2</sup> -MLP-wide [38]	$224 \times 224$	80.0	94.8	71	14
Mixer-B/16 [30]	$224 \times 224$	76.4	–	59	12
Mixer-B/16*	$224 \times 224$	77.2	92.9	59	12
Mixer-B/16*+CCS	$224 \times 224$	79.8	94.6	57	11
S <sup>2</sup> -MLP-deep [38]	$224 \times 224$	80.7	95.4	51	11
ResMLP-36 [31]	$224 \times 224$	79.7	–	44	9
ResMLP-36*	$224 \times 224$	79.8	94.7	44	9
ResMLP-36*+CCS	$224 \times 224$	80.6	95.3	43	9

**Table 4.** Comparisons with other models on ImageNet-1K benchmark without extra data. ViT-B/16\* denotes the result of ViT-B/16 model reported in MLP-Mixer [30] with extra regularization. Mixer-B/16\* and ResMLP-36\* denotes the results of our implementation of Mixer-B/16 [30] and ResMLP-36 [31] based on settings in DeiT [30]. “+CCS” denotes replacing the vanilla token-mixing MLP with the proposed CCS token-mixing MLP.

At last, we compare with MLP-based backbones including FF [25], MLP-mixer [30], ResMLP [31] and S<sup>2</sup>-MLP [38]. To make a fair comparison, we re-implement both MLP-mixer [30] and ResMLP [31] through the same settings as ours and DeiT. As shown in Table 4, using the same settings as ours and DeiT, Mixer-B/16\* and ResMLP-36\* achieve better performance than that in the original papers, Mixer-B/16 [30] and ResMLP-36 [31]. By replacing the vanilla token-mixing MLP with the proposed CCS token-mixing MLP, both MLP-mixer and ResMLP achieve higher recognition accuracy with fewer parameters. To be specific, using the vanilla token-mixing MLP, Mixer-B/16\* only achieves a 77.2% top-1 accuracy with 59M parameters. In contrast, using our CCS token-mixing MLP, we achieve a 79.8% top-1 accuracy with only 57M parameters. Besides, ResMLP-36\* achieves a 79.8% top-1 accuracy with 44M parameters using the vanilla token-mixing MLP. After using our CCS token-mixing MLP, the top-1 accuracy increases to 80.6% with only 43M parameters. In fact, since the number of patches,  $S = 196$ , is not large, using FFT for achieving the multiplication between a vector and a circulant matrix does not bring a considerable reduction in computation cost compared with the vanilla token-mixing MLP. Meanwhile, compared with S<sup>2</sup>-MLP-wide and S<sup>2</sup>-MLP-deep, Mixer-B/16\*+CCS and ResMLP-36\*+CCS achieve comparable recognition accuracy using fewer parameters and FLOPs.

## 5.2 Ablation study

The core hyper-parameter in our CCS token-mixing MLP layer is  $G$ , the number of groups. We show the influence of  $G$  on ResMLP-36+CCS in Table 5. As shown in Table 5, when  $G = 1$ , it achieves a 80.0, which has outperformed the original ResMLP-36\* [31], validating the effectiveness of using circulant structure only. Meanwhile, when  $G$  increases from 1 to 8, the recognition on ImageNet1K consistently improves. This validates the effectiveness of conducting different token-mixing operations on different groups of channels. Besides, when  $G$  further increases from 8 to 384, the recognition accuracy saturates but the number of parameters increases from 43M to 46M. Considering both effectiveness and efficiency, we set the number of groups,  $G = 8$ , by default.

G	1	4	8	384	ResMLP-36* [31]
top-1	80.0	80.4	<b>80.6</b>	<b>80.6</b>	79.8
top-5	95.0	95.1	<b>95.3</b>	<b>95.3</b>	94.7
parameters	43M	43M	43M	46M	44M

**Table 5.** The influence of the number of groups,  $G$ , on the recognition accuracy and the number of parameters. The experiments are conducted on ImageNet1K dataset.

## 6 Conclusion

The token-mixing MLP in the existing MLP-based vision backbone is spatial-specific and channel-agnostic. The spatial-specific configuration makes it sensitive to spatial translation. Meanwhile, the channel-agnostic property limits its capability in mixing tokens. To overcome those limitations, we propose a Circulant Channel-specific (CCS) token-mixing MLP, which is spatial-agnostic and channel-specific. The spatial-agnostic property makes our CCS token-mixing MLP more robust to spatial translation and the channel-specific property enables it to encode richer visual patterns. Meanwhile, by exploiting the circulant structure, the number of parameters in the token-mixing MLP layer is significantly reduced. Experiments on ImageNet1K dataset show that, by replacing existing token-mixing MLPs with our CCS token-mixing MLPs, we achieve higher recognition accuracy with fewer parameters.

## References

1. Jimmy Lei Ba, Jamie Ryan Kiros, and Geoffrey E Hinton. Layer normalization. *arXiv preprint arXiv:1607.06450*, 2016.
2. Andrew Brown, Pascal Mettes, and Marcel Worring. 4-connected shift residual networks. In *Proceedings of the 2019 IEEE/CVF International Conference on Computer Vision (ICCV) Workshops*, pages 1990–1997, Seoul, Korea, 2019.
3. Tianlong Chen, Yu Cheng, Zhe Gan, Lu Yuan, Lei Zhang, and Zhangyang Wang. Chasing sparsity in vision transformers: An end-to-end exploration. *arXiv preprint arXiv:2106.04533*, 2021.
4. François Chollet. Xception: Deep learning with depthwise separable convolutions. In *Proceedings of the 2017 IEEE Conference on Computer Vision and Pattern Recognition (CVPR) 2017*, pages 1800–1807, Honolulu, HI, 2017.
5. Xiangxiang Chu, Zhi Tian, Yuqing Wang, Bo Zhang, Haibing Ren, Xiaolin Wei, Huaxia Xia, and Chunhua Shen. Twins: Revisiting the design of spatial attention in vision transformers. *arXiv preprint arXiv:2104.13840*, 2021.
6. Xiangxiang Chu, Zhi Tian, Bo Zhang, Xinlong Wang, Xiaolin Wei, Huaxia Xia, and Chunhua Shen. Conditional positional encodings for vision transformers. *arXiv preprint arXiv:2102.10882*, 2021.
7. Ekin D. Cubuk, Barret Zoph, Jonathon Shlens, and Quoc V. Le. Randaugment: Practical automated data augmentation with a reduced search space. In *Proceedings of the 2020 IEEE/CVF Conference on Computer Vision and Pattern Recognition (CVPR) Workshops*, pages 3008–3017, Seattle, WA, 2020.
8. Jia Deng, Wei Dong, Richard Socher, Li-Jia Li, Kai Li, and Fei-Fei Li. Imagenet: A large-scale hierarchical image database. In *Proceedings of the 2009 IEEE Computer Society Conference on Computer Vision and Pattern Recognition (CVPR)*, pages 248–255, Miami, FL, 2009.

9. Alexey Dosovitskiy, Lucas Beyer, Alexander Kolesnikov, Dirk Weissenborn, Xi-aohua Zhai, Thomas Unterthiner, Mostafa Dehghani, Matthias Minderer, Georg Heigold, Sylvain Gelly, Jakob Uszkoreit, and Neil Houlsby. An image is worth 16x16 words: Transformers for image recognition at scale. In *Proceedings of the 9th International Conference on Learning Representations (ICLR)*, Virtual Event, 2021.
10. Peng Gao, Jiasen Lu, Hongsheng Li, Roozbeh Mottaghi, and Aniruddha Kembhavi. Container: Context aggregation network. *arXiv preprint arXiv:2106.01401*, 2021.
11. Meng-Hao Guo, Zheng-Ning Liu, Tai-Jiang Mu, and Shi-Min Hu. Beyond self-attention: External attention using two linear layers for visual tasks. *arXiv preprint arXiv:2105.02358*, 2021.
12. Kai Han, An Xiao, Enhua Wu, Jianyuan Guo, Chunjing Xu, and Yunhe Wang. Transformer in transformer. *arXiv preprint arXiv:2103.00112*, 2021.
13. Kaiming He, Xiangyu Zhang, Shaoqing Ren, and Jian Sun. Deep residual learning for image recognition. In *Proceedings of the 2016 IEEE Conference on Computer Vision and Pattern Recognition (CVPR)*, pages 770–778, Las Vegas, NV, 2016.
14. Dan Hendrycks and Kevin Gimpel. Gaussian error linear units (GELUS). *arXiv preprint arXiv:1606.08415*, 2016.
15. Byeongho Heo, Sangdoon Yun, Dongyoon Han, Sanghyuk Chun, Junsuk Choe, and Seong Joon Oh. Rethinking spatial dimensions of vision transformers. *arXiv: 2103.16302*, 2021.
16. Elad Hoffer, Tal Ben-Nun, Itay Hubara, Niv Giladi, Torsten Hoefer, and Daniel Soudry. Augment your batch: Improving generalization through instance repetition. In *Proceedings of the 2020 IEEE/CVF Conference on Computer Vision and Pattern Recognition (CVPR)*, pages 8126–8135, Seattle, WA, 2020.
17. Andrew G Howard, Menglong Zhu, Bo Chen, Dmitry Kalenichenko, Weijun Wang, Tobias Weyand, Marco Andreetto, and Hartwig Adam. Mobilenets: Efficient convolutional neural networks for mobile vision applications. *arXiv preprint arXiv:1704.04861*, 2017.
18. Zilong Huang, Yucheng Ben, Guozhong Luo, Pei Cheng, Gang Yu, and Bin Fu. Shuffle transformer: Rethinking spatial shuffle for vision transformer. *arXiv preprint arXiv:2106.03650*, 2021.
19. Lukasz Kaiser, Aidan N. Gomez, and François Chollet. Depthwise separable convolutions for neural machine translation. In *Proceedings of the 6th International Conference on Learning Representations (ICLR)*, Vancouver, Canada, 2018.
20. Alex Krizhevsky, Ilya Sutskever, and Geoffrey E. Hinton. Imagenet classification with deep convolutional neural networks. In *Advances in Neural Information Processing Systems (NIPS)*, pages 1106–1114, Lake Tahoe, NV, 2012.
21. Gustav Larsson, Michael Maire, and Gregory Shakhnarovich. Fractalnet: Ultra-deep neural networks without residuals. In *Proceedings of the 5th International Conference on Learning Representations (ICLR)*, Toulon, France, 2017.
22. Hanxiao Liu, Zihang Dai, David R So, and Quoc V Le. Pay attention to mlps. *arXiv preprint arXiv:2105.08050*, 2021.
23. Ze Liu, Yutong Lin, Yue Cao, Han Hu, Yixuan Wei, Zheng Zhang, Stephen Lin, and Baining Guo. Swin transformer: Hierarchical vision transformer using shifted windows. *arXiv preprint arXiv:2103.14030*, 2021.
24. Ilya Loshchilov and Frank Hutter. Decoupled weight decay regularization. In *Proceedings of the 7th International Conference on Learning Representations (ICLR)*, New Orleans, LA, 2019.
25. Luke Melas-Kyriazi. Do you even need attention? a stack of feed-forward layers does surprisingly well on imagenet. *arXiv preprint arXiv:2105.02723*, 2021.

26. Ilija Radosavovic, Raj Prateek Kosaraju, Ross B. Girshick, Kaiming He, and Piotr Dollár. Designing network design spaces. In *Proceedings of the 2020 IEEE/CVF Conference on Computer Vision and Pattern Recognition (CVPR)*, pages 10425–10433, Seattle, WA, 2020.
27. Chen Sun, Abhinav Shrivastava, Saurabh Singh, and Abhinav Gupta. Revisiting unreasonable effectiveness of data in deep learning era. In *Proceedings of the IEEE International Conference on Computer Vision (ICCV)*, pages 843–852, Venice, Italy, 2017.
28. Christian Szegedy, Vincent Vanhoucke, Sergey Ioffe, Jonathon Shlens, and Zbigniew Wojna. Rethinking the inception architecture for computer vision. In *Proceedings of the 2016 IEEE Conference on Computer Vision and Pattern Recognition (CVPR)*, pages 2818–2826, Las Vegas, NV, 2016.
29. Mingxing Tan and Quoc V. Le. Efficientnet: Rethinking model scaling for convolutional neural networks. In *Proceedings of the 36th International Conference on Machine Learning (ICML)*, pages 6105–6114, Long Beach, CA, 2019.
30. Ilya Tolstikhin, Neil Houlsby, Alexander Kolesnikov, Lucas Beyer, Xiaohua Zhai, Thomas Unterthiner, Jessica Yung, Andreas Steiner, Daniel Keysers, Jakob Uszkoreit, Mario Lucic, and Alexey Dosovitskiy. MLP-Mixer: An all-MLP architecture for vision. *arXiv preprint arXiv:2105.01601*, 2021.
31. Hugo Touvron, Piotr Bojanowski, Mathilde Caron, Matthieu Cord, Alaeldin El-Nouby, Edouard Grave, Armand Joulin, Gabriel Synnaeve, Jakob Verbeek, and Hervé Jégou. ResMLP: Feedforward networks for image classification with data-efficient training. *arXiv preprint arXiv:2105.03404*, 2021.
32. Hugo Touvron, Matthieu Cord, Matthijs Douze, Francisco Massa, Alexandre Sablayrolles, and Hervé Jégou. Training data-efficient image transformers & distillation through attention. *arXiv preprint arXiv:2012.12877*, 2020.
33. Hugo Touvron, Matthieu Cord, Alexandre Sablayrolles, Gabriel Synnaeve, and Hervé Jégou. Going deeper with image transformers. *arXiv preprint arXiv:2103.17239*, 2021.
34. Ashish Vaswani, Noam Shazeer, Niki Parmar, Jakob Uszkoreit, Llion Jones, Aidan N. Gomez, Lukasz Kaiser, and Illia Polosukhin. Attention is all you need. In *Advances in Neural Information Processing Systems (NIPS)*, pages 5998–6008, Long Beach, CA, 2017.
35. Wenhai Wang, Enze Xie, Xiang Li, Deng-Ping Fan, Kaitao Song, Ding Liang, Tong Lu, Ping Luo, and Ling Shao. Pyramid vision transformer: A versatile backbone for dense prediction without convolutions. *arXiv preprint arXiv:2102.12122*, 2021.
36. Bichen Wu, Alvin Wan, Xiangyu Yue, Peter Jin, Sicheng Zhao, Noah Golmant, Amir Gholaminejad, Joseph Gonzalez, and Kurt Keutzer. Shift: A zero flop, zero parameter alternative to spatial convolutions. In *Proceedings of the IEEE Conference on Computer Vision and Pattern Recognition*, pages 9127–9135, 2018.
37. Haiping Wu, Bin Xiao, Noel Codella, Mengchen Liu, Xiyang Dai, Lu Yuan, and Lei Zhang. CvT: Introducing convolutions to vision transformers. *arXiv preprint arXiv:2103.15808*, 2021.
38. Tan Yu, Xu Li, Yunfeng Cai, Mingming Sun, and Ping Li. S<sup>2</sup>-mlp: Spatial-shift mlp architecture for vision. *arXiv preprint arXiv:2106.07477*, 2021.
39. Li Yuan, Yunpeng Chen, Tao Wang, Weihao Yu, Yujun Shi, Zihang Jiang, Francis EH Tay, Jiashi Feng, and Shuicheng Yan. Tokens-to-token ViT: Training vision transformers from scratch on imagenet. *arXiv preprint arXiv:2101.11986*, 2021.
40. Sangdoon Yun, Dongyoon Han, Sanghyuk Chun, Seong Joon Oh, Youngjoon Yoo, and Junsuk Choe. Cutmix: Regularization strategy to train strong classifiers with

- localizable features. In *Proceedings of the 2019 IEEE/CVF International Conference on Computer Vision (ICCV)*, pages 6022–6031, Seoul, Korea, 2019.
41. Hongyi Zhang, Moustapha Cissé, Yann N. Dauphin, and David Lopez-Paz. mixup: Beyond empirical risk minimization. In *Proceedings of the 6th International Conference on Learning Representations (ICLR)*, Vancouver, Canada, 2018.
  42. Zizhao Zhang, Han Zhang, Long Zhao, Ting Chen, and Tomas Pfister. Aggregating nested transformers. *arXiv preprint arXiv:2105.12723*, 2021.